THE JOURNAL OF PHYSICAL CHEMISTRY A

Article

pubs.acs.org/JPCA

Excited-State Dynamics of Wurster's Salts

Jakob Grilj,[†] Philipp Buchgraber,[‡] and Eric Vauthey*[,†]

[†]Department of Physical Chemistry and [‡]Department of Organic Chemistry, University of Geneva, 30 quai Ernest-Ansermet, CH-1211 Geneva 4

Supporting Information

ABSTRACT: The excited-state dynamics of a series of Wurster's salts (*p*-phenylenediamine radical cations) with different subtituents on the nitrogen atoms was investigated under a variety of experimental conditions using a combination of ultrafast spectroscopic techniques. At room temperature, the lifetime of the lowest excited state of all radical cations is on the order of 200 fs, independently of the solvent, that is, water, nitriles, alcohols, and room-temperature ionic liquid. On the other hand, all cations, except that with the bulky nitrogen substituents, become fluorescent below 120 K. The observed dynamics can be accounted for by the presence of a conical intersection between the D_1 and D_0 states. For the cations with a small nitrogen substituent, this conical intersection could be accessed through a twist of one amino group, as already suggested for Wurster's Blue. However, this coordinate cannot be invoked for the cation with bulky nitrogen subtituents, and more probably, pyramidalization of the nitrogen center and/or deformation of the phenyl ring play an important role. Consequently, the excited-state dynamics of these structurally very similar Wurster's salts involves different decay mechanisms.

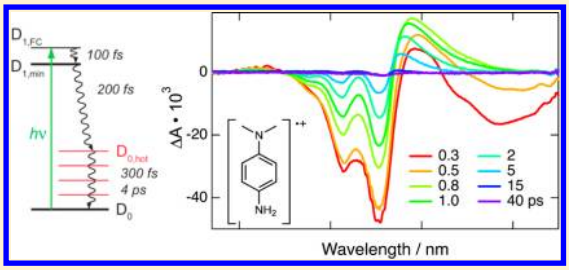

INTRODUCTION

Radical ions are regaining interest nowadays as they are found to be key intermediates in enzyme-catalyzed reactions[1−3] and as their power is being increasingly recognized in biochemical and chemical synthesis.[2,3] Most of our knowledge about radical ions stems from reaction mechanism and electron paramagnetic resonance (EPR) studies, and only little is known about their electronic excited-state dynamics in liquid solution. Ultrafast nonradiative decay of the electronic excited state has been observed in most cases.[4−15] It is commonly argued that this is due to the small energy gap between the D_0 ground state and the D_1 lowest electronic excited state. A small radiative rate constant together with a large nonradiative rate constant and a high probability for state crossings (conical intersections, CIs) favor a nonradiative decay of D_1 and thus a negligibly small fluorescence quantum yield. For example, the radical ions of various polycyclic aromatic hydrocarbons were investigated at room temperature, mainly by transient absorption and transient grating spectroscopy, and D_1 lifetimes ranging between 0.05 and 40 ps were observed.[5,7,9,11−13]

According to quantum chemical calculations, the ultrafast excited-state decay of naphthalene[16] and the pyrene radical cation[17] is due to the presence of planar CIs connecting the excited and ground states. Along the same line, a recent experimental study on the 2,3,5,6-tetrafluoro-7,7,8,8-tetracyanoquinodimethane radical anion indicates that the decay of its D_2 state does not involve major structural changes.[18]

Much longer excited-state lifetimes, up to 500 ps, were reported for some aromatic di- and tetracarboximide anions,[6] but the longest found so far, to our knowledge, amounts to 63 ns and was measured with the 1,4-benzoquinone radical anion in liquid *i*-octane.[19] The D_1 state of these radical anions is located at significantly higher D_1 energy, 1.5 and 2.0 eV, respectively, than that in the examples mentioned before. However, a high-lying D_1 state does not warrant a long lifetime. Indeed, the excited-state lifetime of the methylviologen radical cation amounts to only 0.7 ps in acetonitrile and 0.4 in water, although the D_1 state is at 1.6 eV.[4,8] Similarly, the D_1 state of Wurster's Blue, located 2 eV above the ground state, has a lifetime of 0.2 ps at room temperature.[15] According to quantum chemistry calculations, the ultrafast decay of its D_1 state is associated with the elongation of one of the nitrogen−phenyl bonds and torsional motion around this bond. At a twist angle of 70°, the two lowest potential energy surfaces are degenerate in a D_1/D_0 CI. According to these calculations, distortion of the phenyl ring or the pyradimalization of the nitrogen center is not sufficient to access a low-lying CI.[15]

The present work intends to reveal whether or not the findings for the excited-state dynamics of Wurster's Blue are general and can be applied to other Wurster's salts. To this end, Wurster's salts bearing different substituents at the amino groups and the phenyl core (Scheme 1) were investigated by ultrafast spectroscopy at ambient temperature in a variety of solvents and at liquid nitrogen temperature by fluorescence techniques. We will show that, although these cations are structurally similar, the decay of their D_1 excited state involves different mechanisms.

Received: May 10, 2012
Revised: June 13, 2012
Published: June 14, 2012

Scheme 1. Wurster's Salts[a]

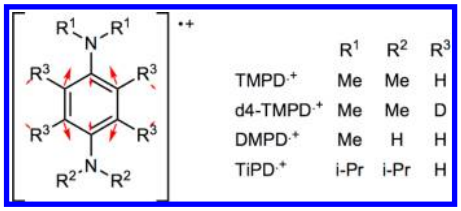

	R1	R2	R3
TMPD•+	Me	Me	H
d4-TMPD•+	Me	Me	D
DMPD•+	Me	H	H
TiPD•+	i-Pr	i-Pr	H

[a]The red arrows illustrate the displacement of atoms in the Franck–Condon-active 8a vibrational mode.

EXPERIMENTAL SECTION

Samples. The *N,N,N′,N′*-tetramethyl-*p*-phenylenediamine radical cation ($TMPD^{\bullet+}$) and *N,N*-dimethyl-*p*-phenylenediamine radical cation ($DMPD^{\bullet+}$) were prepared as perchlorate salts according to the literature.[20] d4-$TMPD^{\bullet+}$ (2,3,5,6-tetradeutero-*N,N,N′,N′*-tetramethyl-*p*-phenylenediamine) was prepared following ref 21 (see the Supporting Information). The synthesis of *N,N,N′,N′*-tetraisopropyl-*p*-phenylenediamine radical cation ($TiPD^{\bullet+}$) is described in the Supporting Information.

For the spectroscopic measurements, methanol (MeOH), ethanol (EtOH), acetonitrile (ACN), and benzonitrile (PhCN) were of analytical grade and used as received from Fluka. Deionized water (H_2O, tap) and deuterated water (D_2O, ARMAR Chemicals) were used as received. The room-temperature ionic liquid (RTIL), 1-ethyl-3-methylimidazolium ethylsulfate (Ecoeng 212, Solvent Innovations), was used as received. Its water content was determined by Karl Fischer titration and amounted to 800 ppm, whereas its viscosity at 20° was 120 cP. To avoid contamination by water, the RTIL was stored in its original cap-sealed flask, and the samples were always under inert atmosphere. For the $DMPD^{\bullet+}$ solutions, the solvents were bubbled with argon for 20 min prior to use to improve sample stability.

Spectroscopic Measurements. Steady-state absorption and emission spectra were recorded on Cary 50 and Cary Eclipse (Varian) spectrometers, respectively. Fluorescence spectra were corrected for the wavelength dependence of detection and transformed according to the literature to judge the mirror image relationship.[22] Low-temperature fluorescence measurements were carried out using an Oxford Instruments Optistat DN cryostat.

The time-correlated single-photon counting (TCSPC) unit is described elsewhere.[23] Excitation was achieved with a 470 nm laser diode (Picoquant LDH-P-C-470), and the Oxford instruments cryostat was fit into the setup. The instrument response function (IRF) had a full width at half-maximum (fwhm) of 320 ps.

The fluorescence up-conversion (FU) setup was essentially the same as that described in ref 24, except for the laser source (MaiTai, Spectra-Physics). The sample was excited at 500 nm, and the fluorescence was up-converted with the polarization of the gate pulse at a magic angle with respect to the pump pulse. The IRF had a fwhm of 200 fs. A rotating sample cell of 1 mm optical path length was used to avoid degradation. Sample stability was checked by absorption spectroscopy prior to and after the up-conversion measurement. The absorbance of the sample was around 0.4 at 500 nm in the 1 mm cell.

The transient absorption (TA) setup has been described in detail elsewhere.[25,26] Pumping was performed either at 550 ($DMPD^{\bullet+}$) or 610 nm (all other samples) using a home-built two-stage noncolinear optical parametric amplifier. These wavelengths ensured that only the cationic form was excited. The pump power at the sample was approximately 0.1 mJ/cm^2. Sample stability was verified by measuring the steady-state absorption spectrum before and after the TA scans. The TA spectra were corrected for the chirp of the white light pulses. The IRF, as deduced from the electronic optical Kerr effect signal, had a fwhm of approximately 200 fs, depending on the wavelength. Note that white light instabilities superimposed a structure on the spectrum above ~700 nm. The accuracy of the lifetimes was around 10%.

RESULTS

The steady-state absorption spectra of the Wurster's salts (Figure 1A) consist of a structured band covering most of the visible region that can be ascribed to the $D_1 \leftarrow D_0$ transition. This transition is associated with a transfer of the charge and unpaired electron from the amino groups toward the phenyl ring.[15] The $D_1 \leftarrow D_0$ band shifts bathochromically with increasing number of alkyl substituents, but the nature of the alkyl group does not play a very significant role, as discussed many years ago by Michaelis and co-workers.[27] The only difference between the absorption spectra of $TMPD^{\bullet+}$ and $TiPD^{\bullet+}$ is a broadening and a 500 cm^{-1} red shift of the latter. From this similarity, including the extinction coefficients,[28] and from EPR[29] and X-ray results,[30] one can safely conclude that $TiPD^{\bullet+}$ has a planar *p*-phenylenediamine center and that the central carbon atom of the *i*-propyl groups are in the phenyl ring plane. The vibrational structure has been identified as the 8a mode (Wilson notation),[31] indicated by the small arrows in Scheme 1.[32,33] This vibrational mode affects the phenyl ring bond lengths and angles but hardly the aromatic hydrogen atoms and the amino groups. Below 400 nm, the absorption spectra exhibit an intense band around 320 nm with a shoulder at longer wavelength. Dichroism measurements have shown that these two features correspond to two distinct electronic

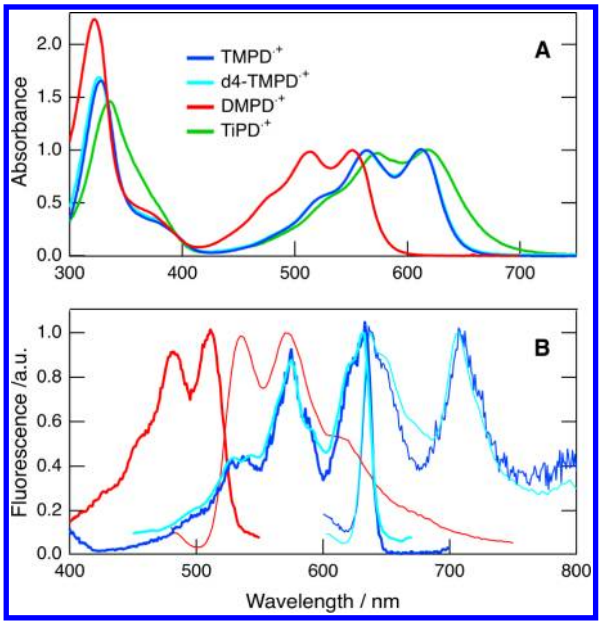

Figure 1. Steady-state spectra of the Wurster's salts in a 1:1 EtOH/MeOH mixture. (A) Absorption at 298 K. (B) Fluorescence emission (thin) and excitation (thick line) at 80 K.

dx.doi.org/10.1021/jp3045548 | J. Phys. Chem. A 2012, 116, 7516–7522

transitions, most probably the $D_3 \leftarrow D_0$ and $D_2 \leftarrow D_0$ transitions.[34]

Upon cooling from 298 to 77 K, the absorption band of the tetra-alkyl salts dissolved in a 1:1 EtOH/MeOH mixture narrows (Figure 1A and B) and undergoes a minor, 250 cm^{-1}, red shift. By contrast, a pronounced, 1400 cm^{-1}, blue shift is observable for $DMPD^{\bullet+}$. Because all four compounds show a similar, small solvatochromism at room temperature that correlates with the refractive index of the solvent and thus arises from dispersion interactions, it is likely that ion pairing in conjunction with hydrogen bonding is responsible for the thermochromic shift of the $DMDP^{\bullet+}$ band. The effect of the counterion on the electronic spectra of ions is well documented.[35] However, the limited sample stability and the tendency of $DMPD^{\bullet+}$ to aggregate at lower temperatures prevented a thorough analysis of this effect.

No stationary fluorescence could be detected at room temperature with all four cations. However, as already found with $TMPD^{\bullet+}$, emission could be recorded below 120 K with all cations but $TiPD^{\bullet+}$, the intensity increasing with further cooling. The emission spectra are the mirror images of the absorption spectra (Figure 1B). The excitation spectra are identical to the absorption spectra except in the UV, where the neutral and the dicationic forms absorb. $DMPD^{\bullet+}$ shows additionally emission from an impurity that is spectrally well-separated and apparently not the dimer (see Figure S1, Supporting Information).[36] Attempts to observe stationary fluorescence with $TiPD^{\bullet+}$ at 12 K were unsuccessful.

The augmentation of fluorescence intensity upon cooling below 120 K correlates with an increased fluorescence lifetime, as measured by TCSPC with $d4\text{-}TMPD^{\bullet+}$. Indeed, whereas the fluorescence decay is faster than the instrument response function above 135 K, the fluorescence lifetime increases from 450 to 640 ps when going from 100 to 78 K. These values are very similar to those found with $TMPD^{\bullet+}$ (Table 1), pointing to an absence of deuterium effect on the nonradiative decay on Wurster's Blue.[15]

Table 1. Fluorescence Lifetimes Recorded in Low-Temperature EtOH/MeOH Glasses

	τ_f/ps	
T/K	d4-$TMPD^{\bullet+}$	$TMPD^{\bullet+}$[a]
78	640	660
90	560	590
100	450	
135	<IRF	<IRF

[a]From ref 15.

The fluorescence dynamics of all Wurster's salts at room temperature was measured in ACN and water by FU. As could be expected from the absence of a measurable steady-state emission, the fluorescence decays within a few hundred femtoseconds only (Figure 2A and Table 2). The fluorescence time profiles measured at different wavelengths were analyzed globally with the sum of exponential functions convolved with the IRF. For $TMPD^{\bullet+}$ and $d4\text{-}TMPD^{\bullet+}$, two exponential functions were sufficient to reproduce the time profiles. The results obtained for these two radical cations are very similar with the shorter time constant, τ_{f1}, around 100 fs and with the amplitude changing from positive, indicating a decay, to negative sign, pointing to a rise, when going from short

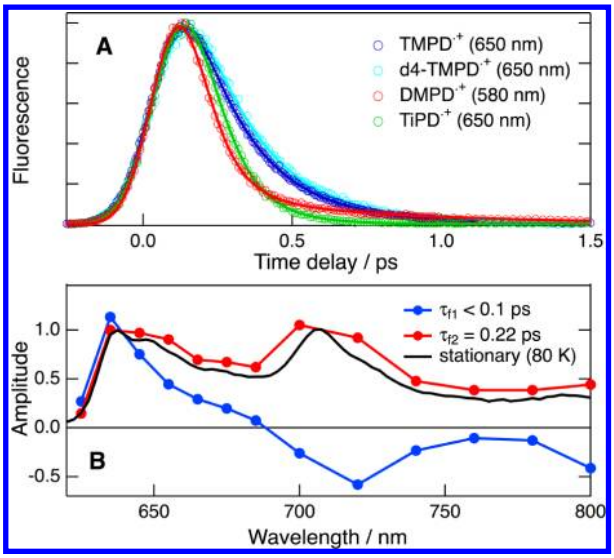

Figure 2. (A) Time profiles of the fluorescence intensity at the wavelength written in parentheses measured with the Wurster's salts in ACN at room temperature. (B) Decay-associated spectra obtained from global analysis of the $d4\text{-}TMPD^{\bullet+}$ data in ACN and the stationary fluorescence spectrum at 80 K.

Table 2. Time Constants Obtained from a Global Multiexponential Analysis of the Fluorescence Time Profiles Measured at Room Temperature[a]

	ACN		D_2O	
cation	τ_{f1}/ps	τ_{f2}/ps	τ_{f1}/ps	τ_{f2}/ps
$TMPD^{\bullet+}$[b]	*0.10*	0.21	*0.10*	0.23
$d4\text{-}TMPD^{\bullet+}$	*0.10*	0.22	*0.12*	0.28
$DMDP^{\bullet+}$[c]	0.10	0.20	0.14	0.66
$TiPD^{\bullet+}$	0.11		0.10	0.80[d]

[a]Values in italic are ascribed to spectral shifts and the others to population decay. [b]From ref 15. [c]Triple exponential decay with an additional 1.5 (ACN) and 8.8 ps (D_2O) component of small amplitude ascribed to fluorescence from a decomposition product. [d]Ascribed to a composition product.

(<700 nm) to long wavelengths. This 100 fs component can thus be interpreted as a red shift of the emission band, most probably due to inertial solvation.[37] The slowest component with a time constant of $\tau_{f2} \approx 250$ fs is associated with a decay at all wavelengths. Therefore, this time constant can be considered as the D_1 excited-state lifetime of $TMPD^{\bullet+}$ and $d4\text{-}TMPD^{\bullet+}$.[38]

The sum of three exponential functions was required to reproduce the data recorded with $DMDP^{\bullet+}$. As the amplitude of the slowest component increased with measurement time, it was ascribed to an emissive decomposition product (Figure S2, Supporting Information). The spectra associated with the other two time constants, $\tau_{f1} \approx 100$ fs and $\tau_{f2} = 0.2–0.6$ ps, exhibit only positive amplitude, suggesting that both components are related to a population decay. As the amplitude of the spectrum associated with τ_{f1} is ~10 times as large as that associated with τ_{f2} (Figure S2, Supporting Information), one can conclude that the 100 fs component makes the main contribution to the excited-state population decay of $DMDP^{\bullet+}$.

For $TiPD^{\bullet+}$, the fluorescence decay can be reproduced with a single-exponential function with a time constant of about 100 fs.

dx.doi.org/10.1021/jp3045548 | J. Phys. Chem. A 2012, 116, 7516–7522

The excited-state dynamics of all four Wurster's salts in various solvents was also investigated by TA spectroscopy, the transient spectra recorded at different time delays after $D_1 \leftarrow D_0$ excitation of $DMPD^{\bullet+}$ and $TiPD^{\bullet+}$ in ACN being shown in Figures 3A and 4A. The spectra measured with

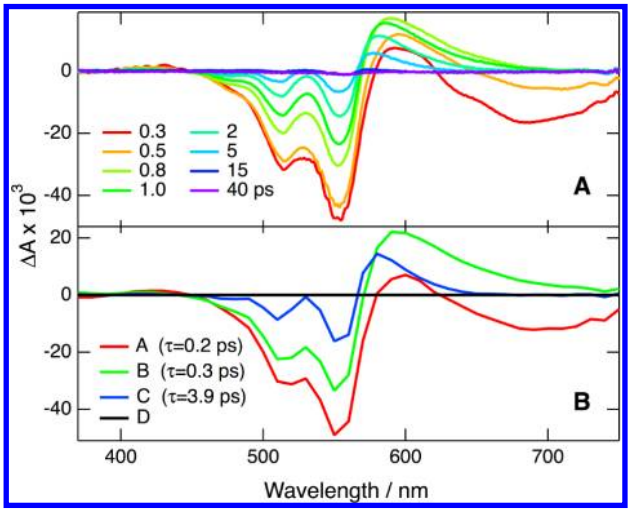

Figure 3. (A) TA spectra recorded at different time delays after 550 nm excitation of $DMPD^{\bullet+}$ in MeOH and (B) evolution-associated difference spectra obtained from target analysis assuming a A → B → C → D scheme.

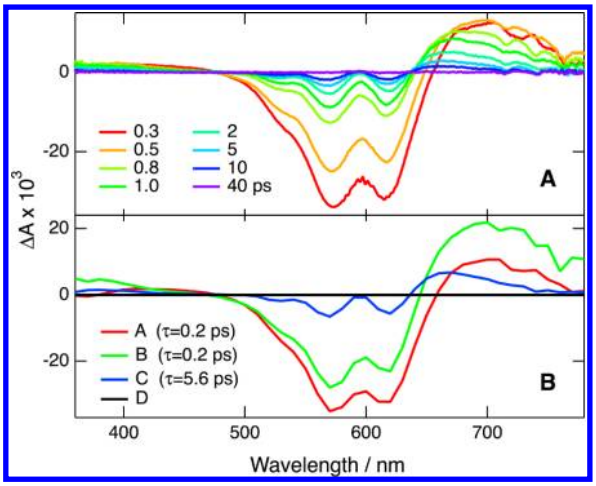

Figure 4. (A) TA spectra recorded at different time delays after 610 nm excitation of $TiPD^{\bullet+}$ in ACN and (B) evolution-associated difference spectra obtained from target analysis assuming a A → B → C → D scheme.

$TPMD^{\bullet+}$, d4-$TMPD^{\bullet+}$, and $DMPD^{\bullet+}$ exhibit similar features, namely, (i) a negative band with a vibrational structure resembling the $D_1 \leftarrow D_0$ absorption band, which can be ascribed to the bleach of this absorption due to the depletion of the ground-state population, (ii) two positive bands at both sides of the ground-state bleach bands, that on the blue side being much weaker, whereas the shape of that on the red side exhibits substantial changes with time, and (iii) a negative band on the red side of the most intense positive TA band that vanishes very quickly and that can be ascribed to $D_1 \rightarrow D_0$ stimulated emission. The TA spectra recorded with $TiPD^{\bullet+}$ exhibit the same features except for the stimulated emission band that is absent (Figure 4A). All TA spectra decay to zero within the time window of the experiment, indicating full recovery of the ground-state population.

To make a more quantitative interpretation of the TA spectra, global multiexponential analysis and target analysis, assuming a succession of first-order steps, were performed. If the number of exponential functions is the same as the number of steps, both approaches yield the same time constants, but the resulting amplitude spectra, namely, decay- and species-associated difference spectra (DADS and SADS, respectively), are different. However, the DADS are linear combinations of the SADS and vice versa.[39] In all cases, three exponential functions, and thus three successive steps (A → B → C → D), were required to properly reproduce the TA dynamics (Table 3 and Figure S3 in the Supporting Information). It should be noted that on this time scale, many processes exhibit nonexponential dynamics, and thus, when performing such an analysis, a given process may contribute to different time constants, and similarly, several processes could be associated with the same time constant. Thus, the interpretation of time constants should be made with caution, and if the time constant increases with each step, it is more appropriate to talk about evolution-associated difference spectra (EADS) than SADS.[39] The fact that, in several cases, the target analysis yields similar values for the first two time constants (Table 3) does not imply that species A and B are identical but merely that they have a similar lifetime. However, as B originates from A, its appearance in the TA spectra is delayed relative to A.

The shortest time constant, τ_{a1}, obtained from the analysis of the TA spectra in ACN and water is very similar to the time constant observed in the FU measurements and ascribed to the excited-state lifetime (Tables 2 and 3). For all compounds but $TiPD^{\bullet+}$, the EADS associated with this decay time contain the $D_1 \rightarrow D_0$ stimulated emission band (Figures 3B and 4B). Therefore, τ_{a1} can be mainly attributed to the decay of the D_1 state population. Other very fast processes, such as solvent and vibrational relaxation, which could be resolved in the FU measurements, could also partially contribute to this time constant. As the lifetime of the D_1 state, τ_{a1}, is close to the IRF, it is not absolutely clear whether the positive band peaking at around 600 nm (Figure 3A) is due to a $D_n \leftarrow D_1$ transition or rather arises from another state populated from D_1. In the case of $TiPD^{\bullet+}$, neither the TA spectra nor the EADS exhibit a stimulated emission band (Figure 4) in agreement with an even shorter D_1 lifetime observed in the fluorescence decay (Table 2). As shown in Table 3, τ_{a1} is quite similar for all four salts; it lies between 200 and 300 fs for both $TMPD^{\bullet+}$ and d4-$TMPD^{\bullet+}$, is slightly shorter between 100 and 200 fs for $DMPD^{\bullet+}$ and $TiPD^{\bullet+}$, and does not exhibit any significant solvent dependence. Although τ_{a1} results from a tail fit to the TA data, it is in good agreement with the τ_f values obtained from the FU profiles, which are in principle more reliable because of the iterative reconvolution procedure used for the analysis. The EADS with the two longer decay times, τ_{a2} and τ_{a3}, have similar shape, with a negative band in the ground-state bleach region and a positive band at longer wavelengths. The latter shifts to the blue when going from the τ_{a2} to the τ_{a3} EADS. These spectra are typical of a vibrationally hot electronic ground state. Indeed, ultrafast internal conversion from the D_1 state populates an excited vibrational state of the D_0 electronic ground state. This vibrational hot ground state, $D_{0,hot}$, absorbs at longer wavelengths relative to D_0 by an amount that increases with the vibrational energy. As vibrational relaxation takes place, the position of the $D_{0,hot}$ absorption band shifts to

dx.doi.org/10.1021/jp3045548 | J. Phys. Chem. A 2012, 116, 7516−7522

Table 3. Time Constants Obtained from a Target Analysis of the TA Spectra in Various Solvents

	H_2O	D_2O	ACN	PhCN	MeOH	EtOH	RTIL
ε_s	78.3	78.3	35.9	25.2	32.7	25.6	27.9
η/cP	1.0	1.0	0.36	1.34	0.59	1.19	120.4
TMPD$^{\bullet+}$[a]							
τ_{a1}/ps	0.23	0.27	0.25	0.29	0.19	0.25	0.25
τ_{a2}/ps	0.22	0.26	0.25	0.30	0.22	0.24	0.33
τ_{a3}/ps	2.7	4.1	4.9	5.8	3.1	4.5	3.0
d4-TMPD$^{\bullet+}$							
τ_{a1}/ps	0.26	0.24	0.23	0.33	0.24	0.24	
τ_{a2}/ps	0.26	0.29	0.26	0.32	0.29	0.23	
τ_{a3}/ps	2.2	3.2	4.7	7.6	3.9	2.5	
DMPD$^{\bullet+}$							
τ_{a1}/ps	0.16	0.10	0.11	0.10	0.24	0.22	
τ_{a2}/ps	0.48	0.52	0.80	1.3	0.29	0.31	
τ_{a3}/ps	2.4	3.7	8.5	10.9	3.9	4.2	
TiPD$^{\bullet+}$							
τ_{a1}/ps	0.18	0.16	0.20	0.11	0.18	0.21	0.22
τ_{a2}/ps	0.20	0.26	0.22	0.30	0.21	0.20	0.35
τ_{a3}/ps	3.6	3.5	5.6	5.7	3.2	3.8	4.8

[a]From ref 15.

shorter wavelengths, accounting for the blue-shifted positive band in the EADS decaying with τ_{a3}. Consequently, τ_{a2} and τ_{a3} reflect the vibrational relaxation dynamics of the hot ground state. This process involves intra- and intermolecular energy-transfer processes and takes place on various time scales, ranging from a few tens of femtoseconds to several picoseconds.[40,41]

DISCUSSION

According to the experimental data, the relaxation dynamics of Wurster's salts upon $D_1 \leftarrow D_0$ excitation can be rationalized in terms of an energy level scheme as that depicted in Figure 5. At

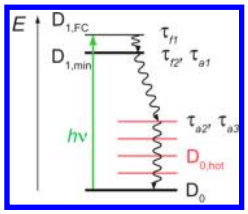

Figure 5. Energy level scheme pertaining to the excited-state dynamics of Wurster's salts and assignment of the measured time constants.

room temperature, the optically populated $D_{1,FC}$ state undergoes ultrafast vibrational/solvent relaxation to $D_{1,min}$. This process is seen by FU with TMPD$^{\bullet+}$ and d4-TMPD$^{\bullet+}$ and is associated with the time constant τ_{f1}. The $D_{1,min}$ population decays on a 100−200 fs time scale ($\tau_{f1,2}$ or τ_{a1}) to a nonfluorescent state, which, according to its TA spectrum, can be assigned to a hot ground state, $D_{0,hot}$. The latter relaxes with a biphasic dynamics (or τ_{a2} and τ_{a3}) back to the thermally equilibrated ground state, D_0. These two time constants, τ_{a2} and τ_{a3}, cannot be ascribed unequivocally to a given relaxation process as they rather reflect an ensemble of intramolecular vibrational energy redistribution, vibrational cooling, and solvation dynamics.

Whereas τ_{a2} exhibits practically no solvent dependence, τ_{a3} is significantly influenced (Table 3). This difference indicates that the shorter of these two time constants is probably dominated by intramolecular vibrational relaxation processes, whereas the longer is most probably related to intermolecular vibrational energy transfer, that is, to vibrational cooling. The solvent dependence of vibrational cooling is still not fully understood. In some cases, a correlation with the thermal diffusivity has been observed.[42,43] Such dependence is however not present here. On the other hand, τ_{a3} is clearly shorter in protic than in aprotic solvents, in agreement with previous investigations that revealed faster cooling in hydrogen-bonding solvents.[40,41]

The ultrafast $D_1 \rightarrow D_0$ relaxation observed with all cations is surprising if one considers the large energy gap between these states, amounting to 2.0 eV for TMPD$^{\bullet+}$, d4-TMPD$^{\bullet+}$, and TiPD$^{\bullet+}$ and 2.2 for DMPD$^{\bullet+}$. Except for TiPD$^{\bullet+}$, the nonradiative decay of the D_1 state is slowed down at low temperature, and consequently, fluorescence becomes competitive. On the other hand, the excited-state lifetime of all Wurster's salts investigated here, with the possible exception of DMPD$^{\bullet+}$ (see below), does not change with solvent properties such as dielectric constant, viscosity, and hydrogen-bond-donating ability. Indeed, with the choice of solvents used, the dielectric constant ranges from 25 in PhCN to 78 in water, the viscosity varies between 0.34 cP in ACN to 120 cP in the RTIL, and the α Kamlet−Taft parameter goes from 0 in PhCN to 1.17 in water.[44]

The time constants found for TMPD$^{\bullet+}$ and d4-TMPD$^{\bullet+}$ are practically the same in all solvents investigated, the discrepancies being ascribed to numerical uncertainties of the fit. This means that the aromatic C−H bonds do not play a significant role in the decay of the D_1 state. This is a clear indication that the nonradiative decay of the D_1 state does not take place via the conventional nuclear tunnelling mechanism, whose efficiency crucially depends on the Franck−Condon factor and thus exhibits a substantial decrease upon perdeuteration.[45] Quantum chemistry calculations performed for TMPD$^{\bullet+}$ confirmed that the ultrafast nonradiative decay of the D_1 state involves a D_1/D_0 CI.[15] This CI is separated from $D_{1,min}$ by a small ($\lesssim$3 kcal·mol^{-1}) barrier that accounts for the increasing D_1 lifetime and the appearance of fluorescence at low temperature. Access to this CI requires a 70° twist of one of the NMe_2 groups. The insensitivity to solvent viscosity was

dx.doi.org/10.1021/jp3045548 | J. Phys. Chem. A 2012, 116, 7516−7522

rationalized by the size of the solvent cage in which the dimethylamino group resides.[15]

This mechanism could also account for the excited-state dynamics of $DMPD^{\bullet+}$, which is also fluorescent at low temperature. Moreover, its shorter D_1 state lifetime relative to $TMPD^{\bullet+}$ (Tables 2 and 3) is compatible with a faster twist of the NH_2 group compared to that of NMe_2. Although the measured lifetimes are close to the IRF, they are the longest in MeOH and EtOH, which have the largest β Kamlet−Taft parameters in the series of solvents used here. This parameter accounts for the hydrogen-bond-accepting basicity of the solvent,[46] and thus, the longer lifetimes could be due to bonds between the NH_2 hydrogens and the alcohols.

On the other hand, the excited-state dynamics of $TiPD^{\bullet+}$ is not compatible with the deactivation mechanism proposed for $TMPD^{\bullet+}$. First, no stationary fluorescence can be observed with this cation even at 12 K. This indicates that there is no barrier between $D_{1,min}$ and the CI responsible for the ultrafast decay. Second, the $N(i\text{-}Pr)_2$ groups are bulkier than the NMe_2 groups, and therefore, a major twist of such groups should not be possible without opposing frictional forces from the solvent. Consequently, this frictional drag should result in an effective barrier for the twist of the $N(i\text{-}Pr)_2$ group, which should increase with solvent viscosity. Such an effect is clearly absent with $TiPD^{\bullet+}$ as the D_1 lifetime amounts to 200 fs in both ACN and the RTIL, although viscosity increases by a factor of ∼350. As outlined before, $TiPD^{\bullet+}$ has a planar *p*-phenylenediamine center, and the central carbon atoms of the *i*-propyl groups are in the same plane as the phenyl ring, and therefore, a "pretwist" of the $N(i\text{-}Pr)_2$ groups cannot be invoked.

The lack of a viscosity dependence of the D_1 lifetime measured by fluorescence could be explained by the need for a small torsion of the amino groups for the excited-state population to exit the FC-active region. However, the TA measurements show that this is not the case because the hot ground state is populated with the same time constant as the fluorescence lifetime. Torsional motion of a NMe_2 group has already been invoked as an important coordinate, like, for example, in the case of the photoinduced intramolecular charge transfer in dimethylamino-benzonitrile (DMABN).[47] However, the charge-transfer time constant changes from 3.7 ps for DMABN in ACN to only 0.9 ps when changing the acceptor unit to benzoic acid ethyl ester, indicating that the measured lifetime does not represent the intrinsic twisting time but is largely controlled by the charge-transfer process itself.[48] As a consequence, it is difficult to estimate whether the viscosity dependence observed for the charge-transfer rate constant arises from twisting motion or is due to solvation dynamics.

A clear viscosity dependence of the nonradiative time constant has been observed in many cases, like, for example, with stilbene,[49] cyanines,[50,51] or triarylmethane dyes.[52,53] The decay time was found to increase with viscosity as $\tau \propto \eta^{\alpha}$, where α was typically between 0.5 and 1.[54] In this cases, however, the volume of the groups undergoing large-amplitude motion was substantially larger than that of a NMe_2 group but similar to that of a $N(i\text{-}Pr)_2$ group, supporting our expectation that torsional motion of a $N(i\text{-}Pr)_2$ group should be viscosity-dependent.

Pyramidalization at a nitrogen center has also been shown to be an important relaxation coordinate for nonradiative deactivation. It is the key step in the $S_1 \rightarrow S_0$ internal conversion of uracil and thymine that takes place in ∼0.1 ps.[55] Moreover, planarization of the NMe_2 group has also been proposed to be the relevant coordinate for the intramolecular charge transfer in DMABN. In this case, no large-amplitude motion is involved, and little dependence on solvent viscosity is expected.[56,57] However, according to the quantum chemistry calculations performed for $TMPD^{\bullet+}$, pyramidalization does not lead to a D_1/D_0 CI.[15]

These examples show some of the mechanisms involved in excited-state interconversion and decay beyond the limit of weak coupling and the difficulties to unequivocally pin down the most relevant coordinate(s). Indeed, the multidimensionality of the evolution of wavepackets and its influence on the photodynamics have been stressed several times.[58−61] It is therefore tenuous to identify the relaxation of a set of molecules with just one coordinate, identical for all of them. The data presented here indicate that even though the structural changes made here do not alter much the properties of the ground state, little can be inferred from this for the excited-state potential energy surface. Whereas the excited-state relaxation of $d4\text{-}TMPD^{\bullet+}$ and $DMPD^{\bullet+}$ agrees with the mechanism proposed for $TMPD^{\bullet+}$, that of $TiPD^{\bullet+}$ involves a different pathway. Pyramidalization of the nitrogen centers is a possible alternative mechanism. Both the neutral TiPD and the cation have planar $N(i\text{-}Pr)_2$ groups, and therefore, if $D_1 \leftarrow D_0$ excitation of $TiPD^{\bullet+}$ leads to a decrease of the phenyl−NR_2 bond order, pyramidalization could become operative and lead to a D_1/D_0 CI. Calculations for $TMPD^{\bullet+}$ indicate that in $D_{1,min}$, the positive charge is localized on the phenyl ring. The latter can thus be expected to be much less rigid than a neutral phenyl ring and easily prone to distortion. In-plane distortion of naphthalene and pyrene cations has been shown to give access to a D_1/D_0 CI.[16,17] Experimentally, the involvement of this mode in the excited-state decay of the Wurster's salt could be tested by investigating cations with methyl substituents on the phenyl ring. Unfortunately, these Wurster's cations are not stable enough for such studies.

CONCLUDING REMARKS

The above results indicate that an ultrashort, solvent-independent excited-state lifetime is a common feature of Wurster's salts but that generalization should be made with care. All radical cations studied here are nonemissive at room temperature, but whereas the nonradiative decay can be slowed down with decreasing temperature for some of them, $TiPD^{\bullet+}$ remains dark even at the lowest temperatures investigated. This and the insensitivity of the D_1 lifetime of $TiPD^{\bullet+}$ to solvent viscosity are evidence that the decay mechanism proposed for $TMPD^{\bullet+}$*, namely, access to a D_1/D_0 CI via a twist of one NMe_2 group, cannot be taken as a general relaxation pathway for Wurster's salts. The excited-state dynamics of $TiPD^{\bullet+}$ should also involve a D_1/D_0 CI, but access to this CI is not limited by a barrier and does not require large-amplitude motion. A detailed computational study of this cation in both ground and excited states could probably give valuable insight into the relaxation pathway. However, such demanding calculations are beyond the scope of this experimental study.

ASSOCIATED CONTENT

Supporting Information

Synthesis of $d4\text{-}TMPD^{\bullet+}$ and $TiPD^{\bullet+}$, low-temperature emission spectrum of $DMDP^{\bullet+}$, decay-associated fluorescence spectra of $DMDP^{\bullet+}$, and global analysis of the TA data measured with $DMDP^{\bullet+}$. This material is available free of charge via the Internet at http://pubs.acs.org.

dx.doi.org/10.1021/jp3045548 | J. Phys. Chem. A 2012, 116, 7516−7522

AUTHOR INFORMATION

Corresponding Author

*E-mail: eric.vauthey@unige.ch.

Notes

The authors declare no competing financial interest.

ACKNOWLEDGMENTS

We would like to thank Mr. Prodita Pal for his help when performing the measurements at 12 K. This project has been supported by the Swiss National Science Foundation (Project 200020-124393) and the University of Geneva.

REFERENCES

(1) Buckel, W. *Angew. Chem., Int. Ed.* **2009**, *48*, 6779−6787.
(2) Ford, L.; Jahn, U. *Angew. Chem., Int. Ed.* **2009**, *48*, 6386−6389.
(3) Yokoyama, K.; Uhlin, U.; Stubbe, J. *J. Am. Chem. Soc.* **2010**, *132*, 15368−15379.
(4) Huang, Y.; Hopkins, J. B. *J. Phys. Chem. A* **1996**, *100*, 9585−9591.
(5) Gumy, J.-C.; Vauthey, E. *J. Phys. Chem. A* **1997**, *101*, 8575−8580.
(6) Gosztola, D.; Niemczik, M. P.; Svec, W.; Lukas, A. S.; Wasielewski, M. R. *J. Phys. Chem. A* **2000**, *104*, 6545−6551.
(7) Brodard, P.; Sarbach, A.; Gumy, J.-C.; Bally, T.; Vauthey, E. *J. Phys. Chem. A* **2001**, *105*, 6594−6601.
(8) Häupl, T.; Lomoth, R.; Hammarström, L. *J. Phys. Chem. A* **2003**, *107*, 435−438.
(9) Zhao, L.; Lian, R.; Shkrob, I. A.; Crowell, R. A.; Pommeret, S.; Chronister, E. L.; Liu, A. D.; Trifunac, A. D. *J. Phys. Chem. A* **2004**, *108*, 25−31.
(10) Okhrimenko, A. N.; Gusev, A. V.; Rodgers, M. A. J. *J. Phys. Chem. A* **2005**, *109*, 7653−7656.
(11) Pagès, S.; Lang, B.; Vauthey, E. *J. Phys. Chem. A* **2006**, *110*, 7547−7553.
(12) Hope, M. J.; Higlett, M. P.; Andrews, D. L.; Meech, S. R.; Hands, I. D.; Dunn, J. L.; Bates, C. A. *Chem. Phys. Lett.* **2009**, *474*, 112−114.
(13) Amarie, S.; Foerster, U.; Gildenhoff, N.; Dreuw, A.; Wachtveitl, J. *Chem. Phys.* **2010**, *373*, 8−14.
(14) Horke, D. A.; Roberts, G. M.; Verlet, J. R. R. *J. Phys. Chem. A* **2011**, *115*, 8369−8374.
(15) Grilj, J.; Laricheva, E. N.; Olivucci, M.; Vauthey, E. *Angew. Chem., Int. Ed.* **2011**, *50*, 4496−4498.
(16) Hall, K. F.; Boggio-Pasqua, M.; Bearpark, M. J.; Robb, M. A. *J. Phys. Chem. A* **2006**, *110*, 13591−13599.
(17) Tokmachev, A. M.; Boggio-Pasqua, M.; Bearpark, M. J.; Robb, M. A. *J. Phys. Chem. A* **2008**, *112*, 10881−10886.
(18) Horke, D. A.; Verlet, J. R. R. *Phys. Chem. Chem. Phys.* **2011**, *13*, 19546−19552.
(19) Cook, A. R.; Curtiss, L. A.; Miller, J. R. *J. Am. Chem. Soc.* **1997**, *119*, 5729−5734.
(20) Michaelis, L.; Schubert, M. P.; Granick, S. *J. Am. Chem. Soc.* **1939**, *61*, 1981−1992.
(21) Giumanini, A. G.; Chiavari, G.; Musiani, M. M.; Rossi, P. *Synthesis* **1980**, 743−746.
(22) Angulo, G.; Grampp, G.; Rosspeintner, A. *Spectrochim. Acta, Part A* **2006**, *65*, 727−731.
(23) Muller, P.-A.; Högemann, C.; Allonas, X.; Jacques, P.; Vauthey, E. *Chem. Phys. Lett.* **2000**, *326*, 321−327.
(24) Morandeira, A.; Engeli, L.; Vauthey, E. *J. Phys. Chem. A* **2002**, *106*, 4833−4837.
(25) Duvanel, G.; Banerji, N.; Vauthey, E. *J. Phys. Chem. A* **2007**, *111*, 5361−5369.
(26) Banerji, N.; Duvanel, G.; Perez-Velasco, A.; Maity, S.; Sakai, N.; Matile, S.; Vauthey, E. *J. Phys. Chem. A* **2009**, *113*, 8202−8212.
(27) Michaelis, L.; Granick, S. *J. Am. Chem. Soc.* **1943**, *65*, 1747−1755.
(28) Rückert, I.; Hebecker, A.; Parusel, A. B. J.; Zachariasse, K. A. *Z. Phys. Chem.* **2000**, *214*, 1597−1597.
(29) Grampp, G.; Kelterer, A.-M.; Landgraf, S.; Sacher, M.; Niethammer, D.; Telo, J. P.; Dias, R. M. B.; Vieira, A. J. S. C. *Monatsh. Chem.* **2005**, *136*, 519−536.
(30) Rosokha, S. V.; Kochi, J. K. *J. Am. Chem. Soc.* **2007**, *129*, 3683−3697.
(31) Wilson, E. B. *Phys. Rev.* **1934**, *45*, 706−706.
(32) Poizat, O.; Bourkba, A.; Buntinx, G.; Deffontaine, A.; Bridoux, M. *J. Chem. Phys.* **1987**, *87*, 6379−6387.
(33) Brouwer, A. M. *J. Phys. Chem. A* **1997**, *101*, 3626−3633.
(34) Albrecht, A. C.; Simpson, W. T. *J. Am. Chem. Soc.* **1955**, *77*, 4454−4461.
(35) Fox, M. A. *Chem. Rev.* **1979**, *79*, 253−273.
(36) Kimura, K.; Yamazaki, T.; Katsumata, S. *J. Phys. Chem.* **1971**, *75*, 1768−1774.
(37) Horng, M. L.; Gardecki, J. A.; Papazyan, A.; Maroncelli, M. *J. Phys. Chem.* **1995**, *99*, 17311−17337.
(38) Fürstenberg, A.; Julliard, M. D.; Deligeorgiev, T. G.; Gadjev, N. I.; Vassilev, A. A.; Vauthey, E. *J. Am. Chem. Soc.* **2006**, *128*, 7661−7669.
(39) van Stokkum, I. H. M.; Larsen, D. S.; van Grondelle, R. *Biochim. Biophys. Acta* **2004**, *1657*, 82−104.
(40) Kovalenko, S. A.; Schanz, R.; Farztdinov, V. M.; Hennig, H.; Ernsting, N. P. *Chem. Phys. Lett.* **2000**, *323*, 312−322.
(41) Pigliucci, A.; Duvanel, G.; Lawson Daku, M. L.; Vauthey, E. *J. Phys. Chem. A* **2007**, *111*, 6135−6145.
(42) Iwata, K.; Hamaguchi, H. *J. Phys. Chem. A* **1997**, *101*, 632−637.
(43) Benniston, A. C.; Matousek, P.; McCulloch, I. E.; Parker, A. W.; Towrie, M. *J. Phys. Chem. A* **2003**, *107*, 4347−4353.
(44) Marcus, Y. *Chem. Soc. Rev.* **1993**, *22*, 409−416.
(45) Kober, E. M.; Caspar, J. V.; Lumpkin, R. S.; Meyer, T. J. *J. Phys. Chem.* **1986**, *90*, 3722−3734.
(46) Kamlet, M. J.; Taft, R. W. *J. Am. Chem. Soc.* **1976**, *98*, 377−383.
(47) Grabowski, Z. R.; Rotkiewicz, K.; Rettig, W. *Chem. Rev.* **2003**, *103*, 3899−4031.
(48) Pigliucci, A.; Vauthey, E.; Rettig, W. *Chem. Phys. Lett.* **2009**, *469*, 115−120.
(49) Velsko, S. P.; Waldeck, D. H.; Fleming, G. R. *J. Chem. Phys.* **1983**, *78*, 249−258.
(50) Sundström, V.; Gillbro, T. *Chem. Phys.* **1981**, *61*, 257−269.
(51) Vauthey, E. *Chem. Phys.* **1995**, *196*, 569−582.
(52) Madge, D.; Windsor, M. W. *Chem. Phys. Lett.* **1974**, *24*, 144−148.
(53) Fita, P.; Punzi, A.; Vauthey, E. *J. Phys. Chem. C* **2009**, *113*, 20705−20712.
(54) Velsko, S. P.; Fleming, G. R. *Chem. Phys.* **1982**, *65*, 59−70.
(55) Gustavsson, T.; Bányász, Á.; Lazzarotto, E.; Markovitsi, D.; Scalmani, G.; Frisch, M. J.; Barone, V.; Improta, R. *J. Am. Chem. Soc.* **2006**, *128*, 607−619.
(56) Chudoba, C.; Kummrow, A.; Dreyer, J.; Stenger, J.; Nibbering, E. T. J.; Elsaesser, T.; Zachariasse, K. A. *Chem. Phys. Lett.* **1999**, *309*, 357−363.
(57) Yoshihara, T.; Druzhinin, S. I.; Zachariasse, K. A. *J. Am. Chem. Soc.* **2004**, *126*, 8535−8539.
(58) Improta, R.; Santoro, F. *J. Chem. Theory Comput.* **2005**, *1*, 215−229.
(59) Hunt, P. A.; Robb, M. A. *J. Am. Chem. Soc.* **2005**, *127*, 5720−5726.
(60) Quenneville, J.; Martínez, T. J. *J. Phys. Chem. A* **2003**, *107*, 829−837.
(61) Olivucci, M.; Sinicropi, A. In *Theoretical and Computational Chemistry*; Olivucci, M., Ed.; Elsevier: New York, 2005; Vol. *16*, pp 1−33.